Volume 16, Number 2, 2023. pp. 169-180

Jordan Journal of Physics

ARTICLE

Effect of Variable Dust Charge on Overtaking Collision of Multi-Solitons in Dusty Plasma

Najah Kabalan, Mahmoud Ahmad and **Ali Asad**

Department of Physics, Faculty of Science, Tishreen University, Latakia, Syria.

Doi: **https://doi.org/10.47011/16.2.5**

Received on: 08/08/2021; Accepted on: 19/09/2021

Abstract: The propagation and overtaking collision of dust acoustic multi-soliton in a dusty plasma consisting of kappa-distributed electrons, Boltzmann-distributed ions, and negatively charged dust grains has been investigated. In the Theoretical study, we use the reductive perturbation method to derive the Korteweg–De Vries (KdV) equation. Using the Hirota bilinear method, we have found four-soliton and five-soliton solutions of the KdV equation. It is observed that the dust charge variation coefficients are significantly affected by the spectral indices of the electrons. We discovered that plasma systems with variable-charged dust grains support the formation of solitons with greater amplitude. Our results help understanding the nonlinear phenomena that form in the magnetospheres of Saturn and Comet Halley as well as in interstellar dusty plasma.

Keywords: Dusty plasma, Overtaking collision, Dust charge variation, Korteweg–De Vries (KdV) equation, Hirota bilinear method.

Introduction

Over the past three decades, numerous wave patterns, interconnected structures along with different instabilities in dusty plasmas, and interaction mechanisms between dust grains and plasma components have attracted the interest of both theoretical and experimental researchers. Their aim being to gain a comprehensive understanding of how these patterns behave in different plasma environments, including planetary rings, the interstellar medium, cometary tails, the surfaces of Mars and the Moon, and the polar mesosphere of Earth [1-3].

Dusty plasma consists of ordinary plasma components, namely electrons and ions, along with charged solid grains. These grains are introduced through various mechanisms, such as the collection of plasma particles, photoionization, and secondary electron emission [1].

Because of the high charge and large mass of the grains relative to ions and electrons, either new or modified wave patterns and instabilities emerge in dusty plasmas, including the dust acoustic (DA) waves, the dust lattice (DL), waves the DIA solitary waves [4], DA solitary waves [5], and the DL solitary waves [6].

In collisionless plasmas, the plasma components are obeying the velocity distribution function that deviates from the Maxwellian distribution. It is observed that the particle velocity distribution function in normal plasma has a high-energy tail [7]. This distribution function is more suitable than the Maxwellian distribution, for it describes particle velocity distributions and is known as the generalized Lorentzian or the kappa distribution. This distribution accurately describes particles with higher velocities when the kappa parameter has specific and small values, and it is given as follows [8]:

$$f(v) = \left[1 + \frac{v^2}{(k\theta)^2}\right]^{-(k+1)} \quad . \tag{1}$$

Corresponding Author: Ali Asad **Email**: ali760633@gmail.com

The kappa distribution has a power-law tail for velocities greater than thermal velocity θ and specific values of the spectral index k. In limit $\rightarrow \infty$, the kappa distribution approximates a Maxwellian distribution.

Kundu et al. [9] investigated the effect of a two-temperature ion on the head-on collision of dust acoustic solitary waves (DASWs) in an unmagnetized dusty plasma with single electrons, two-temperature ions, and variable dust charge. They found that the phase shift is affected by dust charge fluctuation. Varghese et al. [10] studied dust acoustic solitary waves (DASW) in a plasma consisting of two components, namely electrons described by kappa distributions and ions described by Maxwellian distributions, and dust particles with varying charges. The Kadomtsev–Petiashvili (KP) equation was used in their study. They found that amplitudes increase when charges on the dust particles vary. Rabia Amour and Mouloud Tribeche [11] used Tsallis statistical mechanics to study variable charges on dust acoustic solitary waves. They showed the effect of electron nonextensive parameter (q) on the shape of the dust acoustic solitons in dusty plasma. They noticed that for $-1 < q < +1$ the soliton pulse amplitude increases while its width is narrowed as $q \rightarrow 1$. In the case $q > 1$ the opposite result was obtained as electron nonextensivity makes the solitary structure more spiky. S. Gh. Dezfuly and D. Dorranian [12] used the reductive perturbation method to derive the Zakharov–Kuznetsov (ZK) equation. They investigated the effect of the magnetic field, nonthermal ions, and variable dust electric charge on the nonlinear dust acoustic solitary waves in a magnetized dusty plasma. They found that the amplitude of the soliton wave increased and eventually stabilized with an increase in the rate of dust charge variation relative to plasma potential. Moreover, they proved that the external magnetic field influences the shape of the solitons. Kabalan et al. [13] investigated the effect of the structure parameter on overtaking collision between two solitons and three solitons in a strongly coupled dusty plasma system consisting of Maxwellian electrons, ions, and dust grains charged with a negative charge. They found that the amplitude and width of the soliton increase with an increase of the structure parameter and decrease with an increase of the coupling parameter. Modeling results on pulsar wind by Singh et al. [14] showed that the concentration of positrons, relativistic factor, and superthermality of electrons and positrons have a significant influence on the dynamical evolution of IASW pulses. Kaur et al. [15] used the reductive perturbation method to derive the Korteweg–De Vries (KdV), modified KdV (mKdV), and the Gardner equations. Their investigation focused on unmagnetized plasma composed of a positive warm ion fluid, two temperature electrons obeying kappa type distribution and penetrated by a positive ion beam. The researches assert that their findings are important in understanding the properties of nonlinear perturbations that arise in Saturn's magnetosphere, solar wind, pulsar magnetosphere, and other astronomical plasma environments.

No work has been reported in the study of the overtaking collision of four and five dust acoustic solitary waves (DASW) in a five-component cometary plasma. The present study aims to narrow this gap. To achieve this goal, we begin by utilizing the findings presented by Varghese et al. [10] to calculate the parameters γ_1, γ_2 which measure the change of dust charge. Subsequently, we develop a simulation to demonstrate the effect of the changing dust charge on the interaction of four and five solitons in a cometary plasma environment containing two types of electrons and two types of ions. Next, the reductive perturbation method is applied to derive the Korteweg–De Vries (KdV) equation. After that, we use the Hirota bilinear method to obtain multi-solitons solutions. We rely on computer modeling using the Maple program to show the time development of the propagation and interaction of solitons.

Basic Equations

In our study, we investigate a five-component system of dusty cometary plasma. This system consists of variable negatively charged inertial dust grains, two components of electrons with different temperatures described by kappa distributions, lighter (hydrogen) ions, and heavier (oxygen) ions. The latter two components are modeled by Maxwellian distributions. The dust fluid equations that can describe this system are given as follows [10]:

$$\frac{\partial n_d}{\partial t} + \frac{\partial (n_d \vartheta_d)}{\partial x} = 0 \qquad (2)$$

$$\frac{\partial \vartheta_d}{\partial t} + \vartheta_d \frac{\partial \vartheta_d}{\partial x} = Z_d \frac{\partial \Phi}{\partial x} \tag{3}$$

$$\frac{\partial^2 \Phi}{\partial x^2} = Z_d n_d + n_{se} + n_{ce} - n_{li} - n_{hi} \tag{4}$$

where n_d is the dust grain number density normalized by n_{d0}, ϑ_d is the dust fluid velocity normalized by the dust-acoustic speed $C_d = (\frac{Z_d K_B T_{eff}}{m_d})^{1/2}$, Φ is the electrostatic potential normalized by $\frac{e\emptyset}{K_B T_{eff}}$, T_{eff} is the effective temperature defined by:

$$T_{eff} = \frac{Z_{d0} n_{d0}}{\left[\frac{n_{se0}}{T_{se}} + \frac{n_{ce0}}{T_{ce}} + \frac{n_{li0}}{T_{li}} + \frac{n_{hi0}}{T_{hi}}\right]} \tag{5}$$

where T temperatures, (li) lighter hydrogen ions, (hi) heavier oxygen ions, (se) hotter solar electrons, (ce) colder cometary electrons, (0) denotes equilibrium values.

n_{se} and n_{ce} described by kappa distribution, can be written in a normalized form as [8]:

$$n_{se} = \nu_{se}\left(1 - \frac{\beta_{se}\emptyset}{k_{se} - \frac{3}{2}}\right)^{-k_{se} + \frac{1}{2}} \tag{6}$$

$$n_{ce} = \nu_{ce}\left(1 - \frac{\beta_{ce}\emptyset}{k_{ce} - \frac{3}{2}}\right)^{-k_{ce} + \frac{1}{2}} \tag{7}$$

n_{li} and n_{hi} described by the Boltzmann distribution, can be written in a normalized form as:

$$n_{li} = \mu_{li} \exp(-s_{li}\emptyset) \tag{8}$$

$$n_{hi} = \mu_{hi} \exp(-s_{hi}\emptyset) \tag{9}$$

where $\nu_{se} = \frac{n_{se0}}{Z_{d0} n_{d0}}$, $\nu_{ce} = \frac{n_{ce0}}{Z_{d0} n_{d0}}$, $\mu_{li} = \frac{n_{li0}}{Z_{d0} n_{d0}}$, $\mu_{hi} = \frac{n_{hi0}}{Z_{d0} n_{d0}}$, $\beta_{se} = \frac{T_{eff}}{T_{se}}$, $\beta_{ce} = \frac{T_{eff}}{T_{ce}}$, $s_{li} = \frac{T_{eff}}{T_{li}}$, $s_{hi} = \frac{T_{eff}}{T_{hi}}$. Time and space variable are normalized respectively by $\omega_{pd} = (\frac{n_{d0} {Z_d}^2 e^2}{m_d})^{1/2}$ and $\lambda_D = (\frac{K_B T_i}{n_{d0} Z_d e^2})^{1/2}$ ' where ω_{pd} is the plasma frequency, λ_D is dust Debye length, whereas K_B, n_{d0}, e, m_d are the Boltzmann constant, the unperturbed dust grain number density, the electron charge, and dust grain mass, respectively. The dust charge variable Q_d is determined by the charge current balance equation as follows [17-18]:

$$\frac{\partial Q_d}{\partial t} + \vartheta_d \frac{\partial Q_d}{\partial x} = I_{ce} + I_{ce} + I_{li} + I_{hi}\,. \tag{10}$$

Since electrons are faster than ions, the dust grain is generally negatively charged. For the calculation of currents, we assume that the potential of the grain is negatively related to the plasma potential. Thus, the negative dust grains will attract ions and repel the electrons. The current of ions and electrons are defined as follows [19-21]:

$$\left.\begin{aligned} I_{li} &= \pi a^2 n_{li} e \sqrt{\frac{8K_B T_{li}}{\pi m_{li}}}\left(1 - \frac{e\emptyset_p}{K_B T_{li}}\right) \\ I_{hi} &= \pi a^2 n_{hi} e \sqrt{\frac{8K_B T_{hi}}{\pi m_{hi}}}\left(1 - \frac{e\emptyset_p}{K_B T_{hi}}\right) \end{aligned}\right\} \tag{11}$$

$$\left.\begin{aligned} I_{ce} &= -\pi a^2 n_{ce} e \sqrt{\frac{8K_B T_{ce}}{\pi m_e}} \frac{\Gamma(k_{ce}+1)}{\Gamma\left(k_{ce}-\frac{1}{2}\right)} \frac{k_{ce}}{k_{ce}^{\frac{3}{2}}(k_{ce}-1)} \left(1 - \frac{e\emptyset_p}{K_B T_{ce}\left(k_{ce}-\frac{3}{2}\right)}\right)^{-k_{ce}+1} \\ I_{se} &= -\pi a^2 n_{se} e \sqrt{\frac{8K_B T_{se}}{\pi m_e}} \frac{\Gamma(k_{se}+1)}{\Gamma\left(k_{se}-\frac{1}{2}\right)} \frac{k_{se}}{k_{se}^{\frac{3}{2}}(k_{se}-1)} \left(1 - \frac{e\emptyset_p}{K_B T_{se}\left(k_{se}-\frac{3}{2}\right)}\right)^{-k_{se}+1} \end{aligned}\right\} \tag{12}$$

$\emptyset_p$ denotes the dust particle surface potential related to the plasma potential. Comparison of the characteristic time of micrometer-sized dust grains motion $\sim 10^{-3}\, s$ and the dust charging time $\sim 10^{-8} s$, it appears that the motion of the dust grains is not so rapid that the contribution of the electron current to the surface of the grain is equal to that ions current. The balance equation is written as follows:

$$I_{ce} + I_{se} + I_{li} + I_{hi} = 0 \tag{13}$$

Substituting (6-9) and (11-12) into (13) and make some mathematical calculations, we obtain the following equation:

$$\alpha_{li}\,\delta_{li}(1 - s_{li}\Psi)\exp(-\emptyset) + \alpha_{hi}\,\delta_{hi}(1 - s_{hi}\Psi)\exp(-\emptyset) - B_{k(ce)}\left(1 - \frac{\beta_{ce}\Psi}{\left(k_{ce}-\frac{3}{2}\right)}\right)^{-k_{ce}+1}\left(1 - \frac{\beta_{ce}\emptyset}{k_{ce}-\frac{1}{2}}\right)^{-k_{ce}+\frac{1}{2}} - \alpha_{se}\delta_{se}\,B_{k(se)}\left(1 - \frac{\beta_{se}\Psi}{\left(k_{se}-\frac{3}{2}\right)}\right)^{-k_{se}+1}\left(1 - \frac{\beta_{se}\emptyset}{k_{se}-\frac{1}{2}}\right)^{-k_{se}+\frac{1}{2}} = 0 \tag{14}$$

where:

$$B_{k(ce)} = \frac{\Gamma(k_{ce}+1)}{\Gamma\left(k_{ce}-\frac{1}{2}\right)} \frac{k_{ce}}{k_{ce}^{\frac{3}{2}}(k_{ce}-1)},$$

$B_{k(se)} = \frac{\Gamma(k_{se}+1)}{\Gamma\left(k_{se}-\frac{1}{2}\right)} \frac{k_{se}}{k_{se}^{\frac{3}{2}}(k_{se}-1)}$, $\alpha_{li} = \sqrt{\frac{T_{li}\, m_e}{m_{li} T_{ce}}}$, $\alpha_{hi} = \sqrt{\frac{T_{hi}\, m_e}{m_{hi} T_{ce}}}$, $\Psi = \frac{e\emptyset_p}{K_B T_{eff}}$, $\delta_{li} = \frac{\mu_{li}}{\nu_{ce}}$, $\delta_{hi} = \frac{\mu_{hi}}{\nu_{ce}}$, $\delta_{se} = \frac{\nu_{se}}{\nu_{ce}}$, $\alpha_{se} = \sqrt{\frac{T_{se}}{T_{ce}}}$

The normalized dust charge obtained from:

$$Z_d = \frac{\Psi}{\Psi_0} \tag{15}$$

where $\Psi_0 = \Psi(\emptyset = 0)$ is the surface potential on the dust particle with respect to the plasma potential at infinity $(\emptyset = 0)$. Ψ_0 can be determined by substituting $\emptyset = 0$ into Eq. (14) as:

$$\alpha_{li}\, \delta_{li}(1 - s_{li}\Psi_0) + \alpha_{hi}\, \delta_{hi}(1 - s_{hi}\Psi_0) - B_{k(ce)} \left(1 - \frac{\beta_{ce}\Psi}{\left(k_{ce}-\frac{3}{2}\right)}\right)^{-k_{ce}+1} - \alpha_{se}\delta_{se}\, B_{k(se)} \left(1 - \frac{\beta_{se}\Psi}{\left(k_{se}-\frac{3}{2}\right)}\right)^{-k_{se}+1} \tag{16}$$

Substituting (15) into (12), $\emptyset$, Z_d are expanded in powers of ε, we obtain:

$$Z_{d1} = \gamma_1\, \emptyset_1 \tag{17}$$

$$Z_{d2} = \gamma_1 \emptyset_2 + \gamma_2\, \emptyset_1^2 \tag{18}$$

Where

$$\gamma_1 = -\frac{1}{\Psi_0}\frac{\gamma_b}{\gamma_a}$$

$$\gamma_a = A_1 + A_2\beta + A_3\beta_{1ce}\left(\frac{k_{ce}-\frac{3}{2}}{k_{ce}}\right)^{\frac{1}{2}}\left(\frac{k_{ce}-\frac{1}{2}}{k_{ce}-\frac{3}{2}}\right)\left(1 - \frac{\beta_{1ce}s\Psi_0}{k_{ce}-\frac{3}{2}}\right)^{-k_{ce}} + A_4\beta_{1se}\left(\frac{k_{se}-\frac{3}{2}}{k_{se}}\right)^{\frac{1}{2}}\left(\frac{k_{se}-\frac{1}{2}}{k_{se}-\frac{3}{2}}\right)\left(1 - \frac{\beta_{1se}s\Psi_0}{k_{se}-\frac{3}{2}}\right)^{-k_{se}}$$

$$\gamma_b = A_1(1 - s\Psi_0) + A_2\beta(1 - \beta s\Psi_0) + A_3\beta_{1ce}\left(\frac{k_{ce}-\frac{3}{2}}{k_{ce}}\right)^{\frac{1}{2}}\left(\frac{k_{ce}-\frac{1}{2}}{k_{ce}-\frac{3}{2}}\right)\left(1 - \frac{\beta_{1ce}s\Psi_0}{k_{ce}-\frac{3}{2}}\right)^{-k_{ce}+1} + A_4\beta_{1se}\left(\frac{k_{se}-\frac{3}{2}}{k_{se}}\right)^{\frac{1}{2}}\left(\frac{k_{se}-\frac{1}{2}}{k_{se}-\frac{3}{2}}\right)\left(1 - \frac{\beta_{1se}s\Psi_0}{k_{se}-\frac{3}{2}}\right)^{-k_{se}+1}$$

where:

$s = \mu_{li}, \beta = \frac{\mu_{hi}}{s}, \beta_{1ce} = \frac{s_{ce}}{s}, \beta_{1se} = \frac{s_{se}}{s}$

$$\gamma_2 = \frac{1}{2\Psi_0}\frac{s(\gamma_{c1}+\gamma_{c2}+\gamma_{c3})}{\gamma_a}$$

$$\gamma_{c1} = A_1(1 - s\Psi_0) + A_2\beta^2(1 - \beta s\Psi_0) - A_3\beta_{1ce}^2\left(\frac{k_{ce}-\frac{3}{2}}{k_{ce}}\right)^{\frac{1}{2}}\left(\frac{\left(k_{ce}-\frac{1}{2}\right)\left(k_{ce}+\frac{1}{2}\right)}{\left(k_{ce}-\frac{3}{2}\right)^2}\right)\left(1 - \frac{\beta_{1ce}s\Psi_0}{k_{ce}-\frac{3}{2}}\right)^{-k_{ce}+1} - A_4\beta_{1se}^2\left(\frac{k_{se}-\frac{3}{2}}{k_{se}}\right)^{\frac{1}{2}}\left(\frac{\left(k_{se}-\frac{1}{2}\right)\left(k_{se}+\frac{1}{2}\right)}{\left(k_{se}-\frac{3}{2}\right)^2}\right)\left(1 - \frac{\beta_{1se}s\Psi_0}{k_{se}-\frac{3}{2}}\right)^{-k_{se}+1}$$

$$\gamma_{c2} = 2\gamma_1\Psi_0\left(A_1 + A_2\beta^2 - A_3\beta_{1ce}^2\left(\frac{k_{ce}-\frac{3}{2}}{k_{ce}}\right)^{\frac{1}{2}}\left(\frac{\left(k_{ce}-\frac{1}{2}\right)(k_{ce}-1)}{\left(k_{ce}-\frac{3}{2}\right)^2}\right)\left(1 - \frac{\beta_{1ce}s\Psi_0}{k_{ce}-\frac{3}{2}}\right)^{-k_{ce}} - A_4\beta_{1se}^2\left(\frac{k_{se}-\frac{3}{2}}{k_{se}}\right)^{\frac{1}{2}}\left(\frac{\left(k_{se}-\frac{1}{2}\right)(k_{se}-1)}{\left(k_{se}-\frac{3}{2}\right)^2}\right)\left(1 - \frac{\beta_{1se}s\Psi_0}{k_{se}-\frac{3}{2}}\right)^{-k_{se}}\right)$$

$$\gamma_{c3} = -(\gamma_1\Psi_0)^2\left(A_3\beta_{1ce}^2\left(\frac{k_{ce}-\frac{3}{2}}{k_{ce}}\right)^{\frac{1}{2}}\left(\frac{k_{ce}(k_{ce}-1)}{\left(k_{ce}-\frac{3}{2}\right)^2}\right)\left(1 - \frac{\beta_{1ce}s\Psi_0}{k_{ce}-\frac{3}{2}}\right)^{-k_{ce}-1} + A_4\beta_{1se}^2\left(\frac{k_{se}-\frac{3}{2}}{k_{se}}\right)^{\frac{1}{2}}\left(\frac{k_{se}(k_{se}-1)}{\left(k_{se}-\frac{3}{2}\right)^2}\right)\left(1 - \frac{\beta_{1se}s\Psi_0}{k_{se}-\frac{3}{2}}\right)^{-k_{se}-1}\right)$$

where $A_1 = \alpha_{li}\, \delta_{li}$, $A_2 = \alpha_{hi}\, \delta_{hi}$, $A_3 = B_{k(ce)}$, $A_4 = \alpha_{se}\, \delta_{se} B_{k(se)}$

Are physical parameters describing of the dust charge variable, when $\gamma_1 = 0$, $\gamma_2 = 0$ we get a fixed dust charge.

Derivation of Kdv equations

Now, we derive the KdV equations from Eqs. (2) and (4) by employing the reductive perturbation method. The independent variables are stretched as [23]:

$$\left.\begin{aligned} \xi = \varepsilon^{\frac{1}{2}}(x-ct);\ \tau = \varepsilon^{\frac{3}{2}}t \\ \frac{\partial}{\partial x} = \varepsilon^{\frac{1}{2}}\frac{\partial}{\partial \xi};\ \frac{\partial}{\partial t} = -c\varepsilon^{\frac{1}{2}}\frac{\partial}{\partial \xi} + \varepsilon^{\frac{3}{2}}\frac{\partial}{\partial \tau}\end{aligned}\right\} \quad (19)$$

The dependent variables are expanded as:

$$\begin{aligned} n_d &= 1 + \varepsilon n_1 + \varepsilon^2 n_2 + \cdots \\ \vartheta_d &= \varepsilon\vartheta_1 + \varepsilon^2\vartheta_2 + \cdots \\ \Phi &= \varepsilon\Phi_1 + \varepsilon^2\Phi_2 + \cdots \\ Z_d &= 1 + \varepsilon Z_{d1} + \varepsilon^2 Z_{d2} + \cdots \end{aligned} \quad (20)$$

where $0 < \varepsilon \ll 1$ is a small perturbation parameter measuring the strength of nonlinearity, substituting (19) (20) into (2) (4) and taking the terms in different powers of ε, we obtain in the lowest order of $\varepsilon^{\frac{3}{2}}$ and ε:

$$-c\frac{\partial n_1}{\partial \xi} + \frac{\partial \vartheta_1}{\partial \xi} = 0 \quad (21)$$

$$-c\frac{\partial \vartheta_1}{\partial \xi} = \frac{\partial \Phi_1}{\partial \xi} \quad (22)$$

$$n_1 + \left(\gamma_1 + \frac{\nu_{se}\beta_{se}(2k_{se}-1)}{2k_{se}-3} + \frac{\nu_{ce}\beta_{ce}(2k_{ce}-1)}{2k_{ce}-3} + s_{li}\mu_{li} + s_{hi}\mu_{hi}\right)\Phi_1 = 0 \quad (23)$$

By solving equations (18) - (20), we obtain the following set of equations:

$$n_1 = -\left(\gamma_1 + \frac{\nu_{se}\beta_{se}(2k_{se}-1)}{2k_{se}-3} + \frac{\nu_{ce}\beta_{ce}(2k_{ce}-1)}{2k_{ce}-3} + s_{li}\mu_{li} + s_{hi}\mu_{hi}\right)\Phi_1 \quad (24)$$

$$\vartheta_1 = -c\left(\gamma_1 + \frac{\nu_{se}\beta_{se}(2k_{se}-1)}{2k_{se}-3} + \frac{\nu_{ce}\beta_{ce}(2k_{ce}-1)}{2k_{ce}-3} + s_{li}\mu_{li} + s_{hi}\mu_{hi}\right)\Phi_1 \quad (25)$$

where c the phase velocity given as follows:

$$c = \sqrt{\frac{1}{\left(\gamma_1 + \frac{\nu_{se}\beta_{se}(2k_{se}-1)}{2k_{se}-3} + \frac{\nu_{ce}\beta_{ce}(2k_{ce}-1)}{2k_{ce}-3} + s_{li}\mu_{li} + s_{hi}\mu_{hi}\right)}} \quad (26)$$

Similarly, We get from the terms of order ε^2 and $\varepsilon^{5/2}$:

$$-c\frac{\partial n_2}{\partial \xi} + \frac{\partial n_1}{\partial \tau} + n_1\frac{\partial \vartheta_1}{\partial \xi} + \frac{\partial \vartheta_2}{\partial \xi} + \vartheta_1\frac{\partial n_1}{\partial \xi} = 0 \quad (27)$$

$$-c\frac{\partial \vartheta_2}{\partial \xi} + \frac{\partial \vartheta_1}{\partial \tau} + \vartheta_1\frac{\partial \vartheta_1}{\partial \xi} = \frac{\partial \Phi_2}{\partial \xi} + \gamma_1\Phi_1\frac{\partial \Phi_1}{\partial \xi} \quad (28)$$

$$\begin{aligned}\frac{\partial^2 \Phi_1}{\partial \xi^2} = {} & n_2 + \left(\gamma_1 + \frac{\nu_{se}\beta_{se}(2k_{se}-1)}{2k_{se}-3} + \frac{\nu_{ce}\beta_{ce}(2k_{ce}-1)}{2k_{ce}-3} + s_{li}\mu_{li} + s_{hi}\mu_{hi}\right)\Phi_2 + \Bigg(-\gamma_1\Big(\gamma_1 + \frac{\nu_{se}\beta_{se}(2k_{se}-1)}{2k_{se}-3} + \frac{\nu_{ce}\beta_{ce}(2k_{ce}-1)}{2k_{ce}-3} + s_{li}\mu_{li} + \\ & s_{hi}\mu_{hi}\Big) + \frac{\beta_{se}^2\nu_{se}(2k_{se}-1)^2}{2(2k_{se}-3)^2} + \frac{\beta_{ce}^2\nu_{ce}(2k_{ce}-1)^2}{2(2k_{ce}-3)^2} - \frac{s_{li}^2\mu_{li}}{2} - \frac{s_{hi}^2\mu_{hi}}{2} + \gamma_2\Bigg)\emptyset_1^2 \end{aligned} \quad (29)$$

By common solution to system of Eqs. (27)-(29), we obtain the following Korteweg–De Vries (KdV) equation for the first-order perturbed electrostatic potential Φ_1 as follows:

$$\frac{\partial \Phi_1}{\partial \tau} + A\Phi_1\frac{\partial \Phi_1}{\partial \xi} + B\frac{\partial^3 \Phi_1}{\partial \xi^3} = 0 \quad (30)$$

where the nonlinear coefficient $\boldsymbol{A}$ and the dispersion coefficient $\boldsymbol{B}$ are given by:

$$A = -\frac{c^3}{2}\left(\frac{3}{c^4} - \frac{2\gamma_1}{c^2} + \frac{\beta_{se}^2\nu_{se}(2k_{se}-1)^2}{2(2k_{se}-3)^2} + \frac{\beta_{ce}^2\nu_{ce}(2k_{ce}-1)^2}{2(2k_{ce}-3)^2} - \frac{s_{li}^2\mu_{li}}{2} - \frac{s_{hi}^2\mu_{hi}}{2} + \gamma_2\right)$$

$$B = \frac{c^3}{2}$$

Multi - solitons Solutions

For obtain multi -soliton solution of Eq. (30) and to study the interaction between them. To do so, we shall employ the Hirota bilinear method [24]:

The first step: Using the transformation in Eq. (30):

$$\Phi_1 = \frac{12B}{A}\frac{\partial^2(\ln(f(\xi,\tau)))}{\partial \xi^2} \quad (31)$$

We get the following equation:

$$-f_\xi f_\tau + ff_{\xi\tau} + Bff_{\xi\xi\xi\xi} - 4Bf_{\xi\xi\xi}.f_\xi + 3B(f_{\xi\xi})^2 = 0 \quad (32)$$

By using the Hirota D-operator, we get:

$$D_\tau D_\xi\{f,f\} = 2(ff_{\xi\tau} - f_\xi f_\tau) \quad (33)$$

$$BD_\xi{}^4\{f,f\} = 2(Bff_{\xi\xi\xi\xi} - 4Bf_\xi f_{\xi\xi\xi} + 3B(f_{\xi\xi})^2) \quad (34)$$

Using (33) and (34) in (32), we get the Hirota bilinear form:

$$(D_\tau D_\xi + BD_\xi{}^4)\{f,f\} = 0 \quad (35)$$

where D is a binary operator (because it operates on a pair of functions) and is called the Hirota derivative.

To get a four-solitons solution of KdV equation we insert $f = 1 + f_1 + f_2 + f_3 + f_4$ where $f_1 = e^{\theta_1} + e^{\theta_2} + e^{\theta_3} + e^{\theta_4}$. To determine f_2, f_3 and f_4 we perform some mathematical calculations getting thereby the following relationships:

$$f_2 = a(1,2)e^{\theta_1+\theta_2} + a(1,3)e^{\theta_1+\theta_3} + a(1,4)e^{\theta_1+\theta_4} + a(2,3)e^{\theta_2+\theta_3} + a(2,4)e^{\theta_2+\theta_4} + a(3,4)e^{\theta_3+\theta_4}$$

$$f_3 = b(1,2,3)e^{\theta_1+\theta_2+\theta_3} + b(1,2,4)e^{\theta_1+\theta_2+\theta_4} + b(1,3,4)e^{\theta_1+\theta_3+\theta_4} + b(2,3,4)e^{\theta_2+\theta_3+\theta_4}$$

$$f_4 = c(1,2,3,4)e^{\theta_1+\theta_2+\theta_3+\theta_4}$$

where:

$$a(1,2) = \frac{(k_1-k_2)^2}{(k_1+k_2)^2}, a(1,3) = \frac{(k_1-k_3)^2}{(k_1+k_3)^2},$$

$$a(1,4) = \frac{(k_1-k_4)^2}{(k_1+k_4)^2}, a(2,3) = \frac{(k_2-k_3)^2}{(k_2+k_3)^2},$$

$$a(2,4) = \frac{(k_2-k_4)^2}{(k_2+k_4)^2}, a(3,4) = \frac{(k_3-k_4)^2}{(k_3+k_4)^2}$$

$$b(1,2,3) = a(1,2)\, a(1,3)\, a(2,3),$$

$$b(1,3,4) = a(1,3)\, a(1,4)\, a(3,4),$$

$$b(2,3,4) = a(2,3)\, a(2,4)\, a(3,4),$$

$$c(1,2,3,4) = a(1,2)\, a(1,3)\, a(1,4)\, a(2,3)\, a(2,4)\, a(3,4)$$

Substituting in Eq. (31), we get the four-soliton solution as follows:

$$\Phi_1 = \frac{12B}{A}\frac{\partial^2}{\partial\xi^2}\{\ln[1 + e^{\theta_1} + e^{\theta_2} + e^{\theta_3} + e^{\theta_4} + a(1,2)e^{\theta_1+\theta_2} + a(1,3)e^{\theta_1+\theta_3} + a(1,4)e^{\theta_1+\theta_4} + a(2,3)e^{\theta_2+\theta_3} + a(2,4)e^{\theta_2+\theta_4} + a(3,4)e^{\theta_3+\theta_4} + b(1,2,3)e^{\theta_1+\theta_2+\theta_3} + b(1,2,4)e^{\theta_1+\theta_2+\theta_4} + b(1,3,4)e^{\theta_1+\theta_3+\theta_4} + b(2,3,4)e^{\theta_2+\theta_3+\theta_4} + c(1,2,3,4)e^{\theta_1+\theta_2+\theta_3+\theta_4}]\} \quad (36)$$

$$\theta_i = k_i B^{-\frac{1}{3}}\xi - k_i^3\tau - \Delta_i; i = 1,2,3,4,$$

$$\Delta_1 = \mp\frac{2B^{\frac{1}{3}}}{k_1}\, ln\left|\sqrt{\frac{c(1,2,3,4)}{a(2,3)\, a(2,4)\, a(3,4)}}\right|;$$

$$\Delta_2 = \mp\frac{2B^{\frac{1}{3}}}{k_2}\, ln\left|\sqrt{\frac{c(1,2,3,4)}{a(1,3)\, a(1,4)\, a(3,4)}}\right|;$$

$$\Delta_3 = \mp\frac{2B^{\frac{1}{3}}}{k_3}\, ln\left|\sqrt{\frac{c(1,2,3,4)}{a(1,2)\, a(1,4)\, a(2,4)}}\right|;$$

$$\Delta_4 = \mp\frac{2B^{\frac{1}{3}}}{k_4}\, ln\left|\sqrt{\frac{c(1,2,3,4)}{a(1,2)\, a(1,3)\, a(2,3)}}\right|$$

To get a five-solitons solution of KdV equation we insert $f = 1 + f_1 + f_2 + f_3 + f_4 + f_5$ where $f_1 = e^{\theta_1} + e^{\theta_2} + e^{\theta_3} + e^{\theta_4} + e^{\theta_5}$. By conducting mathematical calculations, we obtain the following relationships to determine f_2, f_3, f_4 and f_5 :

$$f_2 = a(1,2)e^{\theta_1+\theta_2} + a(1,3)e^{\theta_1+\theta_3} + a(1,4)e^{\theta_1+\theta_4} + a(1,5)e^{\theta_1+\theta_5} + a(2,3)e^{\theta_2+\theta_3} + a(2,4)e^{\theta_2+\theta_4} + a(2,5)e^{\theta_2+\theta_5} + a(3,4)e^{\theta_3+\theta_4} + a(3,5)e^{\theta_3+\theta_5} + a(4,5)e^{\theta_4+\theta_5}$$

$$f_3 = b(1,2,3)e^{\theta_1+\theta_2+\theta_3} + b(1,2,4)e^{\theta_1+\theta_2+\theta_4} + b(1,2,5)e^{\theta_1+\theta_2+\theta_5} + b(1,3,4)e^{\theta_1+\theta_3+\theta_4} + b(1,3,5)e^{\theta_1+\theta_3+\theta_5} + b(1,4,5)e^{\theta_1+\theta_4+\theta_5} + b(2,3,4)e^{\theta_2+\theta_3+\theta_4} + b(2,3,5)e^{\theta_2+\theta_3+\theta_5} + b(2,4,5)e^{\theta_2+\theta_4+\theta_5} + b(3,4,5)e^{\theta_3+\theta_4+\theta_5}$$

$$f_4 = c(1,2,3,4)e^{\theta_1+\theta_2+\theta_3+\theta_4} + c(1,2,3,5)e^{\theta_1+\theta_2+\theta_3+\theta_5} + c(1,2,4,5)e^{\theta_1+\theta_2+\theta_4+\theta_5} + c(1,3,4,5)e^{\theta_1+\theta_3+\theta_4+\theta_5} + c(2,3,4,5)e^{\theta_2+\theta_3+\theta_4+\theta_5}$$

$$f_5 = d(1,2,3,4,5)e^{\theta_1+\theta_2+\theta_3+\theta_4+\theta_5}$$

where:

$$a(1,2) = \frac{(k_1-k_2)^2}{(k_1+k_2)^2}, a(1,3) = \frac{(k_1-k_3)^2}{(k_1+k_3)^2},$$

$$a(1,4) = \frac{(k_1-k_4)^2}{(k_1+k_4)^2}, a(1,5) = \frac{(k_1-k_5)^2}{(k_1+k_5)^2},$$

$$a(2,3) = \frac{(k_2-k_3)^2}{(k_2+k_3)^2}, a(2,4) = \frac{(k_2-k_4)^2}{(k_2+k_4)^2},$$

$$a(2,5) = \frac{(k_2-k_5)^2}{(k_2+k_5)^2}, a(3,4) = \frac{(k_3-k_4)^2}{(k_3+k_4)^2},$$

$$a(3,5) = \frac{(k_3-k_5)^2}{(k_3+k_5)^2}, a(4,5) = \frac{(k_4-k_5)^2}{(k_4+k_5)^2}$$

$$b(1,2,3) = a(1,2)\, a(1,3)\, a(2,3),$$

$$b(1,3,4) = a(1,3)\, a(1,4)\, a(3,4),$$

$$b(1,3,5) = a(1,3)\, a(1,5)\, a(3,5),$$

$$b(1,2,4) = a(1,2)\, a(1,4)\, a(2,4),$$

$$b(1,2,5) = a(1,2)\, a(1,5)\, a(2,5),$$

$$b(1,4,5) = a(1,4)\, a(1,5)\, a(4,5),$$

$b(2,3,4) = a(2,3)\ a(2,4)\ a(3,4),$

$b(2,3,5) = a(2,3)\ a(2,5)\ a(3,5),$

$b(2,4,5) = a(2,4)\ a(2,5)\ a(4,5),$

$b(3,4,5) = a(3,4)\ a(3,5)\ a(4,5)$

$c(1,2,3,4) = a(1,2)\ a(1,3)\ a(1,4)\ a(2,3)\ a(2,4)\ a(3,4),$

$c(1,2,3,5) = a(1,2)\ a(1,3)\ a(1,5)\ a(2,3)\ a(2,5)\ a(3,5),$

$c(1,2,4,5) = a(1,2)\ a(1,4)\ a(1,5)\ a(2,4)\ a(2,5)\ a(4,5),$

$c(1,3,4,5) = a(1,3)\ a(1,4)\ a(1,5)\ a(3,4)\ a(3,5)\ a(4,5),$

$c(2,3,4,5) = a(2,3)\ a(2,4)\ a(2,5)\ a(3,4)\ a(3,5)\ a(4,5),$

$d(1,2,3,4,5) = a(1,2)\ a(1,3)\ a(1,4)\ a(1,5)\ a(2,3)\ a(2,4)\ a(2,5)\ a(3,4)\ a(3,5)\ a(4,5)$

Substituting in Eq. (31), we get the five - soliton solution as follows:

$$\Phi_1 = \frac{12B}{A}\frac{\partial^2}{\partial\xi^2}\{\ln[1 + e^{\theta_1} + e^{\theta_2} + e^{\theta_3} + e^{\theta_4} + e^{\theta_5} + a(1,2)e^{\theta_1+\theta_2} + a(1,2)e^{\theta_1+\theta_2} + a(1,3)e^{\theta_1+\theta_3} + a(1,4)e^{\theta_1+\theta_4} + a(1,5)e^{\theta_1+\theta_5} + a(2,3)e^{\theta_2+\theta_3} + a(2,4)e^{\theta_2+\theta_4} + a(2,5)e^{\theta_2+\theta_5} + a(3,4)e^{\theta_3+\theta_4} + a(3,5)e^{\theta_3+\theta_5} + a(4,5)e^{\theta_4+\theta_5} + b(1,2,3)e^{\theta_1+\theta_2+\theta_3} + b(1,2,4)e^{\theta_1+\theta_2+\theta_4} + b(1,2,5)e^{\theta_1+\theta_2+\theta_5} + b(1,3,4)e^{\theta_1+\theta_3+\theta_4} + b(1,3,5)e^{\theta_1+\theta_3+\theta_5} + b(1,4,5)e^{\theta_1+\theta_4+\theta_5} + b(2,3,4)e^{\theta_2+\theta_3+\theta_4} + b(2,3,5)e^{\theta_2+\theta_3+\theta_5} + b(2,4,5)e^{\theta_2+\theta_4+\theta_5} + b(3,4,5)e^{\theta_3+\theta_4+\theta_5} + c(1,2,3,4)e^{\theta_1+\theta_2+\theta_3+\theta_4} + c(1,2,3,5)e^{\theta_1+\theta_2+\theta_3+\theta_5} + c(1,2,4,5)e^{\theta_1+\theta_2+\theta_4+\theta_5} + c(1,3,4,5)e^{\theta_1+\theta_3+\theta_4+\theta_5} + c(2,3,4,5)e^{\theta_2+\theta_3+\theta_4+\theta_5} + d(1,2,3,4,5)e^{\theta_1+\theta_2+\theta_3+\theta_4+\theta_5}]\} \quad (37)$$

where:

$$\theta_i = k_i B^{-\frac{1}{3}}\xi - k_i^3\tau - \Delta_i'; i = 1,2,3,4,5$$

$$\Delta_1' = \mp\frac{2B^{\frac{1}{3}}}{k_1}\ ln\left|\sqrt{\frac{d(1,2,3,4)}{a(2,3)\ a(2,4)\ a(2,5)\ a(3,4)\ a(3,5)\ a(4,5)}}\right|$$

$$\Delta_2' = \mp\frac{2B^{\frac{1}{3}}}{k_2}\ ln\left|\sqrt{\frac{d(1,2,3,4,5)}{a(1,3)\ a(1,4)\ a(1,5)a(3,4)\ a(3,5)\ a(4,5)}}\right|$$

$$\Delta_3' = \mp\frac{2B^{\frac{1}{3}}}{k_3}\ ln\left|\sqrt{\frac{d(1,2,3,4,5)}{a(1,2)\ a(1,4)a(1,5)\ a(2,4)a(2,5)a(4,5)}}\right|$$

$$\Delta_4' = \mp\frac{2B^{\frac{1}{3}}}{k_4}\ ln\left|\sqrt{\frac{d(1,2,3,4,5)}{a(1,2)\ a(1,3)\ a(1,5)a(2,3)\ a(2,5)a(3,5)}}\right|$$

$$\Delta_5' = \mp\frac{2B^{\frac{1}{3}}}{k_5}\ ln\left|\sqrt{\frac{d(1,2,3,4,5)}{a(1,2)\ a(1,3)\ a(1,4)a(2,3)a(2,4)a(3,4)}}\right|$$

Discussion and Conclusion

In this section, numerical analysis has been performed to study the properties overtaking collision of four-solitons and five-solitons under the influence of dust charge variation with other fixed physical parameters. The results of the Rosetta spacecraft observations of Comet 67P/Churyumov–Gerasimenko were used [16]. The effect of dust charge variation coefficients on phase shifts and time evolution of multi-solitons is demonstrated in the following section.

Time Evolution of Multi –Solitons:

Fig. 1 demonstrates time evaluation of the interaction of rarefactive four-solitons. When solitons are moving in the same direction but at different speeds, solitons with larger amplitudes tend to have higher speeds. The velocity of a soliton is proportional to its amplitude, while the width of a soliton is inversely proportional to the square root of its amplitude, which means that longer solitons are much thinner than shorter solitons. At $\tau = -1$ the larger amplitude soliton is behind small amplitude soliton. Over time, the solitons get closer to each other and merge into a single soliton at $\tau = 0$. But at $\tau = 1$ the solitons separate again, and each soliton returns to its original shape before the collision. A larger amplitude soliton comes to the fore.

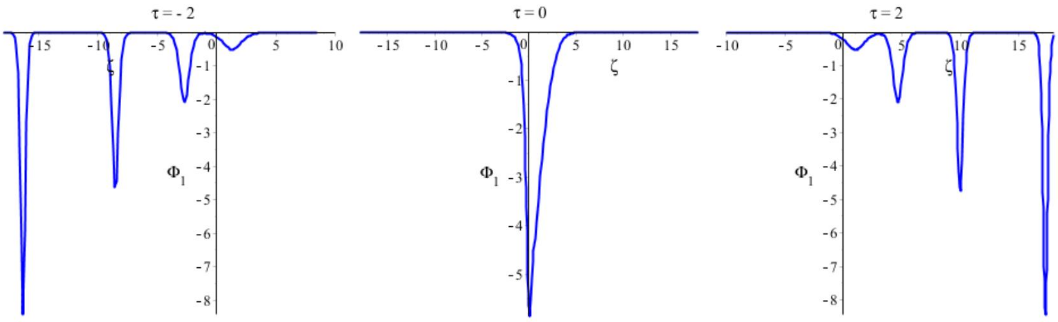

FIG. 1. Time evolution of four – solitons at different times, $k_1 = 1, k_2 = 2, k_3 = 3, k_4 = 4$.

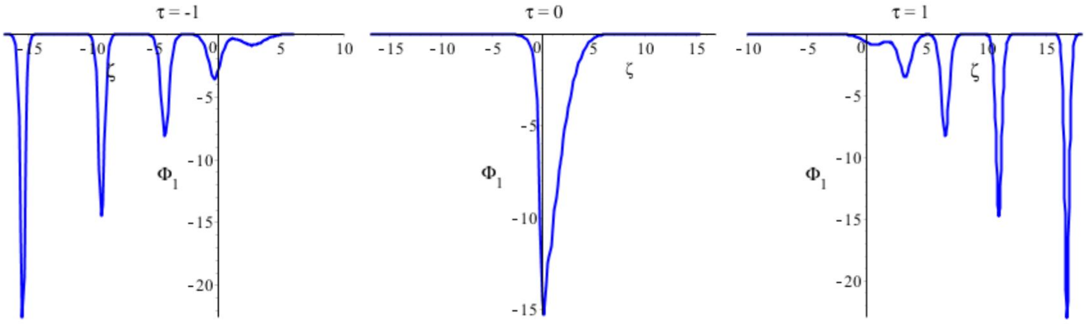

FIG. 2. Time evolution of five – solitons at different times, $k_1 = 1, k_2 = 2, k_3 = 3, k_4 = 4, k_5 = 5$.

It is clear from the figures that the solitons regain their original shapes and velocities after the collision.

The effects of dispersion in the plasma medium lead to the disintegration of a single soliton, with the larger soliton appearing first, followed by the smaller soliton, and then the even smaller ones.

Solitons maintain their original profile before interaction due to the balance between the effects of nonlinearity and dissipation. Solitons are similar in their behavior to particles in that they maintain their profiles despite interacting with each other.

Previous investigations on the overtaking and head-on collision between solitary waves showed that collisions are accompanied by deviations known as phase shifts [24, 25]. In other words, the trajectories of the solitons after the collision deviate from their trajectories before the collision.

The obtained results align with the findings reported previously, as well as with the results concerning the interaction of two solitons and three solitons. [25-28].

Soliton Shape Changes

In this section, we study the effect of varying charges on a grain's surface and the spectral indices $\mathrm{k}_{ce}, \mathrm{k}_{se}$ on the profile of the interacting solitons. Fig.s 3(a) and 4(a) show the change in the profile of the four-solitons and five-solitons for two different values of $\mathrm{k}_{ce}, \mathrm{k}_{se}$ at $\tau = -1$ with varying charge.

Figs. 3(b) and 4(b) show the changes in the form of four-solitons and five-solitons for the constant dust charge $\gamma_1, \gamma_2 = 0$, varying dust charge $\gamma_1, \gamma_2 \neq 0$, and fixed values for spectral indices $\mathrm{k}_{ce}, \mathrm{k}_{se} = 3$. It was found that there is a small increase in the amplitude of the solitons in case of varying dust charge.

The amplitude is sure to increase due to the change in nonlinear and dispersive effects under the influence of varying dust charges. Eventually, a large increase in amplitude causes steepening of the dust acoustic solitary waves and produces a new type of linear wave called a dust acoustic shockwave. These patterns have been observed in all comets [29].

On the other hand, we found that the amplitudes of solitons increase with increasing values of spectral indices $\mathrm{k}_{ce}, \mathrm{k}_{se}$ (i.e., decrease in the superthermality of the two types of electrons).

Both types of high-energy electrons (low values of spectral indices) provide more energy to the motion of the studied solitons, causing an increase in their velocities and, thus, an increase in their amplitudes. Similar results have been presented in other studies [10, 29].

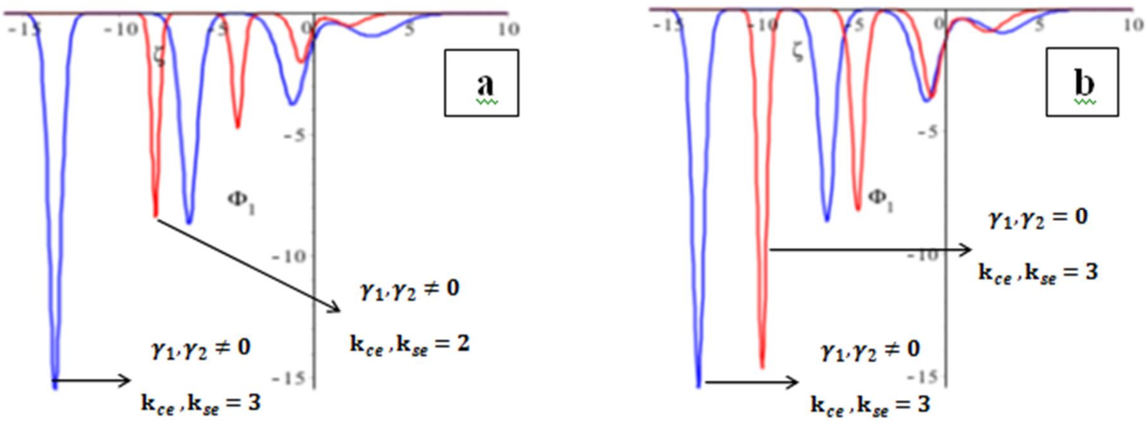

FIG. 3. Four - solitons shape variations for different values of spectral indices k_{ce}, k_{se} and variable dust charge. Other parameters are: $n_{d0} = 0.05\ cm^{-3}, Z_{d0} = 200, n_{hi0} = 0.5\ cm^{-3}, n_{li0} = 4.95\ cm^{-3}, T_{ce} = 2 \times 10^4\ K, T_{se} = 2 \times 10^5\ K, m_{li} = 1.67 \times 10^{-24}\ g, m_{hi} = 16 \times 1.67 \times 10^{-24}\ g, m_e = 9.1 \times 10^{-28}\ g, T_{li} = 8 \times 10^4\ K, T_{hi} = 2.8 \times 10^4\ K$.

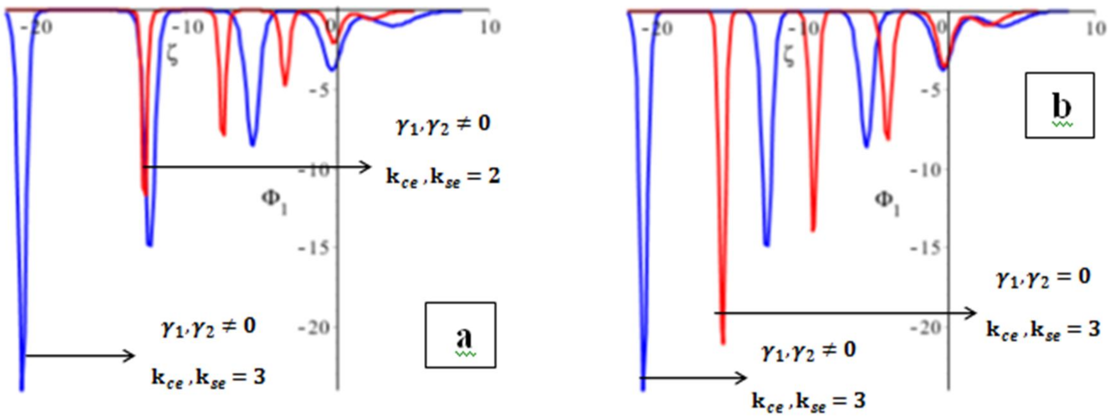

FIG. 4. Five - solitons shape variations for different values of spectral indices k_{ce}, k_{se} and variable dust charge. Other parameters are: $n_{d0} = 0.05\ cm^{-3}, Z_{d0} = 200, n_{hi0} = 0.5\ cm^{-3}, n_{li0} = 4.95\ cm^{-3}, T_{ce} = 2 \times 10^4\ K, T_{se} = 2 \times 10^5\ K, m_{li} = 1.67 \times 10^{-24}\ g, m_{hi} = 16 \times 1.67 \times 10^{-24}\ g, m_e = 9.1 \times 10^{-28}\ g, T_{li} = 8 \times 10^4\ K, T_{hi} = 2.8 \times 10^4\ K$.

Figs. 5(a) and 5(b) show the changes in the form of four-solitons and five-solitons with colder electrons $n_{ce0} = 5\ cm^{-3}, T_{ce} = 2 \times 10^4 K$ as well as without colder electrons $n_{ce0} = 0\ cm^{-3}, T_{ce} = 0K$. It was found that the presence of a new type of electron contributes to a decrease in the amplitude of solitons.

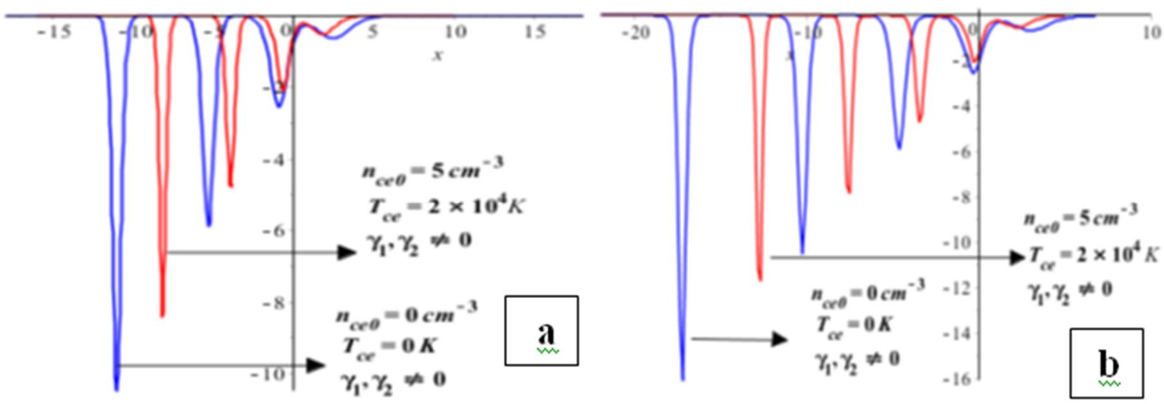

FIG. 5. Four- and five - solitons shape variations for different values of n_{ce0}, T_{ce} and variable dust charge. Other parameters are: $n_{d0} = 0.05\ cm^{-3}, Z_{d0} = 200, n_{hi0} = 0.5\ cm^{-3}, n_{li0} = 4.95\ cm^{-3}, T_{se} = 2 \times 10^5\ K, m_{li} = 1.67 \times 10^{-24}\ g, m_{hi} = 16 \times 1.67 \times 10^{-24}\ g, m_e = 9.1 \times 10^{-28}\ g, T_{li} = 8 \times 10^4\ K, T_{hi} = 2.8 \times 10^4\ K, k_{se} = 2$.

Phase Shifts

The results of the simulation of the interaction between solitons showed that each soliton maintains its original shape before the reaction. This fact has been demonstrated in previous studies for the interaction of two-solitons and three-solitons and in this work for the interaction of four-solitons and five-solitons.

Fig. 6 shows the phase shift changes Δ_1 $(k_1 = 1)$ against k_{ce} for a constant dust charge $\gamma_1, \gamma_2 = 0$ and a varying dust charge $\gamma_1, \gamma_2 \neq 0$. It has been shown that the phase shifts increase with increasing k_{ce}. On the other hand, it is shown that for large values of k_{ce}, the phase shifts are significantly increased in the case $\gamma_1, \gamma_2 \neq 0$.

The phase shift of the soliton occurs as a result of the consumption of its energy during the collision. In other words, the consumption of the energy of the soliton during the reaction increases with the increase of spectral indices and varying dust charges.

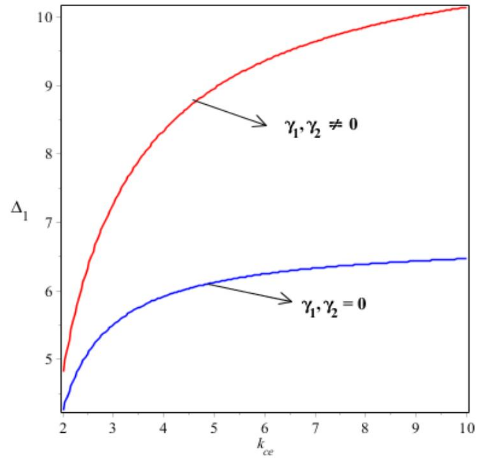

FIG. 6. Variation of the phase shift Δ_1 against the spectral indices k_{ce} for $\gamma_1, \gamma_2 = 0$ and $\gamma_1, \gamma_2 \neq 0$. Other parameters are: $n_{d0} = 0.05\ cm^{-3}, Z_{d0} = 200, n_{hi0} = 0.5\ cm^{-3}, n_{li0} = 4.95\ cm^{-3}, T_{ce} = 2 \times 10^4\ K, T_{se} = 2 \times 10^5\ K, m_{li} = 1.67 \times 10^{-24}\ g, m_{hi} = 16 \times 1.67 \times 10^{-24}\ g, m_e = 9.1 \times 10^{-28}\ g, T_{li} = 8 \times 10^4\ K, T_{hi} = 2.8 \times 10^4\ K, k_{se} = 2, k_1 = 1$.

Figs. 7 and 8 show the phase shifts changes against the spectral indices k_{ce} for four-solitons $(k_1 = 1, k_2 = 2, k_3 = 3, k_4 = 4)$ and five-solitons $(k_1 = 1, k_2 = 2, k_3 = 3, k_4 = 4, k_5 = 5)$.

We noted that the phase shifts of small solitons are greater than that of large solitons. The reason is that the large solitons force the small ones to delay in appearance after the collision. This result is consistent with previous experimental and theoretical work [25-29].

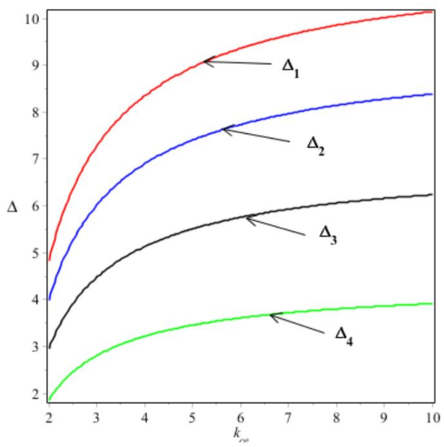

FIG. 7. Variation of the phase shift of Four - solitons against the spectral indices k_{ce} for $k_1 = 1, k_2 = 2, k_3 = 3, k_4 = 4$. Other parameters are: $n_{d0} = 0.05\ cm^{-3}, Z_{d0} = 200, n_{hi0} = 0.5\ cm^{-3}, n_{li0} = 4.95\ cm^{-3}, T_{ce} = 2 \times 10^4\ K, T_{se} = 2 \times 10^5\ K, m_{li} = 1.67 \times 10^{-24}\ g, m_{hi} = 16 \times 1.67 \times 10^{-24}\ g, m_e = 9.1 \times 10^{-28}\ g, T_{li} = 8 \times 10^4\ K, T_{hi} = 2.8 \times 10^4\ K, k_{se} = 2$

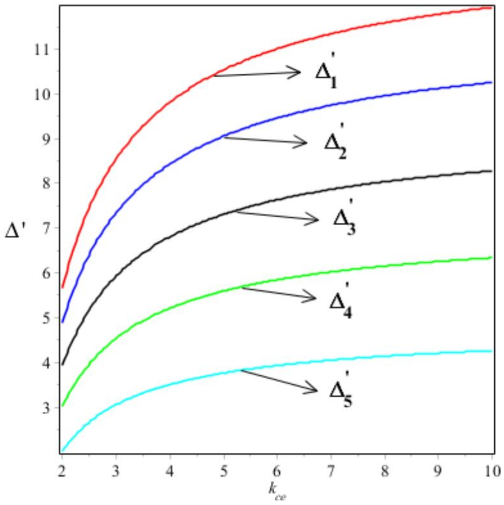

FIG. 8. Variation of the phase shift of five-solitons against the spectral indices k_{ce} for $k_1 = 1, k_2 = 2, k_3 = 3, k_4 = 4, k_5 = 5$. Other parameters are: $n_{d0} = 0.05\ cm^{-3}, Z_{d0} = 200, n_{hi0} = 0.5\ cm^{-3}, n_{li0} = 4.95\ cm^{-3}, T_{ce} = 2 \times 10^4\ K, T_{se} = 2 \times 10^5\ K, m_{li} = 1.67 \times 10^{-24}\ g, m_{hi} = 16 \times 1.67 \times 10^{-24}\ g, m_e = 9.1 \times 10^{-28}\ g, T_{li} = 8 \times 10^4\ K, T_{hi} = 2.8 \times 10^4\ K, k_{se} = 2$.

Conclusions

In this study, we investigated the overtaking collision of dust acoustic multi-soliton in a dusty plasma consisting of variable negatively charged inertial dust grains, components of electrons with different temperatures described by kappa distributions, a lighter (hydrogen) ion component, and a heavier (oxygen) ion component. As a first step, we have derived the Korteweg–De Vries (KdV) equation. Next, applying the Hirota direct method, we have presented four-soliton and five-soliton solutions of the KdV equation. Moreover, we used the results of the observations of Comet 67P/Churyumov–Gerasimenko to model two types of electrons: the hotter solar electrons, on the one hand, and the colder cometary electrons, on the other. It has been observed that a larger soliton moves faster, approaches a smaller solitons, and recovers its original shape and speed after the collision. The amplitude of four-soliton and five-soliton increases when the charges on the dust particles vary. The phase shift of solitons increases with increasing of spectral indices. The increase is significant when the charges on the dust particles vary for large values of spectral indices.

The presence of new superthermal components in the plasma contributes to a significant modification of the surface charge of the dust grains, which leads to a decrease in the amplitude of oscillation.

Hirota's method differs from previous studies in terms of the type of collision it focuses on. Specifically, Hirota's method examines the overtaking collision of multi-solitons, whereas the Poincaré–Lighthill–Kuo method analyzes head-on collisions between solitons. [29]. Both methods agree on the relationship between the phase shifts of solitons and the cube root of the dispersion coefficient B, as well as their amplitudes. This study is important for understanding many nonlinear phenomena in space and astronomical plasma environments, including cometary dusty plasma, Saturn's rings, and interstellar clouds [30, 18].

Acknowledgments

This study was supported by Tishreen University.

References:

[1] Goertz, C.K., Rev. Geophys., 27 (1989) 271.

[2] Goertz, C.K., Rev. Geophys., 27 (2) (1989) 21.

[3] Havnes, O., Melanso, F., Hoz, C.L. and Aslaksen, T., Phys. Scripta, 45 (5) (1992) 433.

[4] Melands, F., Phys. Plasmas, 3 (11) (1996) 11.

[5] Amin, M.R., Morfill, G.E. and Shukla, P.K., physical review, 58 (5) (1998) 6.

[6] Mamun, A.A. and Shukla, P.K., Phys. of Plasmas, 10 (11) (2003) 8.

[7] Pierrard, V., Lazar, M., Solar Phys., 267 (2010) 21.

[8] Hau, L.N. and Fu, W.Z., Phys. Plasmas, 14 (2007) 110702.

[9] Kundu, S.K., Chatterjee, P. and Ghosh, U.N., Astrophys Space Sci., 340 (2012) 5.

[10] Varghese, A., Saritha, A.C., Willington, N.T., Michael, S. and Sreekala, M.S., J. Astrophys. Astr., 41 (11) (2020).

[11] Amour, R. and Tribeche, M., Phys. Plasmas, 17 (2010) 063702.

[12] Dezfuly, S.Gh. and Dorranian, D., Contrib. Plasma Phys., 53 (8) (2013) 8.

[13] Kabalan, N., Ahmad, M. and Asad, A., Advances in Mathematical Phys., 2020 (2020) 9.

[14] Singh, K., Kakad, A., Kakad, B. and Saini, N.S., Monthly Notices of the Royal Astronomical Society, 500 (2) (2021) 8.

[15] Kaur, N., Singh, K. and Saini, N.S., Phys. of Plasmas, 24 (2017) 092108.

[16] Eriksson, A.I., Engelhardt, I.A.D., André, M., Boström, R., Edberg, N.J.T., Johansson, F.L. and Odelstad, E., Astronomy & Astrophysics, 605 (15) (2018) 14.

[17] Su, C.H. and Mirie, R.M., J. Fluid Mech., 98 (1980) 509.

[18] Bandyopadhyay, P., Prasad, G., Sen, A. and Kaw, P.K., Phys. Rev. Lett., 101 (2008) 065006.

[19] Klein, U. and Kerp, J., "Argelander", (Institut fur Astronomie, Bonn, 2008).

[20] Dorranian, D. and Sabetkar, A., Phys. Plasmas, 19 (2012) 013702.

[21] Naeem, I., Ehsan, Z., Mirza, A.M. and Murtaza, G., Phys. of Plasmas, 27 (2020) 043703.

[22] Abid, A.A., Ali, S., Du, J. and Mamun, A.A., Phys. Plasmas, 22 (2015) 084507.

[23] Singh, K., Sethi, P. and Saini, N.S., Phys. of Plasmas, 25 (2018) 033705.

[24] Hirota, R., "The Direct Method in Soliton Theory", (Cambridge Tracts in Mathematics, No. 155, 2004).

[25] Boruah, A., Sharma, S.K., Nakamura, Y. and Bailung, H., Phys. of Plasmas, 23 (9) (2016) 7.

[26] Asita, S. and Prasanta, C., Astrophys. Space Sci., 353 (2014) 8.

[27] Roy, K., Maji, T.K. and Ghorui, M.K., Astrophys Space Sci., 352 (2014) 6.

[28] Mandal, G., Roy, K., Paul, A., Saha, A. and Chatterjee, P., Z. Naturforsch., 70 (2015) 8.

[29] Naeem, I., Ehsan, Z., Mirza, A.M. and Murtaza, G., 2001 (1) (2020) 09374.

[30] Goertz, C.K., Linhua-Shan and Havnes, O., Geophys. Res. Lett., 15 (84) (1988).